# THE MASSIVE CORE OF W51

D. T. JAFFE,[1,2] E. E. BECKLIN,[2,3] AND R. H. HILDEBRAND[4]
*Received 1983 November 7; accepted 1983 December 20*

## ABSTRACT

We have mapped the submillimeter continuum emission from the region around W51 with 40″ resolution. The emission peaks on the $H_2O$ maser emission center W51 MAIN and has a secondary maximum near the compact H II region/20 μm source W51 IRS 2. This is in contrast to the far-IR emission distribution which peaks strongly on IRS 2. The submillimeter and far-IR results together show that, while IRS 2 dominates the luminosity distribution, most of the molecular material in W51 surrounds W51 MAIN. The submillimeter results imply a total mass for the W51 molecular cloud of approximately $10^5 M_\odot$, one-fourth of which lies within 20″ (0.7 pc) of the source center. The mean $H_2$ density over this inner region is approximately $2 \times 10^5$ cm$^{-3}$. The core mass is therefore $\geq 500$ times the Jeans mass for this region. The visual extinction toward the peak of the source is $\geq 10^3$ mag. This large value may explain the nondetection of 20 μm emission from the powerful $H_2O$ maser emission centers and compact H II regions near the submillimeter peak.

*Subject headings:* infrared: sources — nebulae: H II regions

## I. INTRODUCTION

W51 is a luminous, well-studied H II region complex in the Sagittarius spiral arm. Kinematic and $H_2O$ Maser proper motion determinations of the distance to W51 place it approximately 7 kpc from the Sun (Bieging 1975; Downes *et al.* 1980; Genzel *et al.* 1981; Schneps *et al.* 1981). The bright extended H II region has a 20 μm counterpart (W51 IRS 1; Wynn-Williams, Becklin, and Neugebauer 1974) and three associated compact H II regions; W51e1, W51e2, and W51d (Scott 1978; Genzel *et al.* 1982). These compact H II regions all have nearby centers of $H_2O$ maser emission which coincide with 2″–3″ diameter clumps of $NH_3$ emission with brightness temperatures of 50–100 K in the (3,3) inversion transition (Forster *et al.* 1978; Moran 1981, as quoted in Genzel *et al.* 1982; Ho, Genzel, and Das 1983). The maser center near W51d (W51 NORTH) coincides with a bright (~ 100 Jy at 20 μm) 2–20 μm source W51 IRS 2 (EAST) (Genzel *et al.* 1982). The two remaining maser centers (W51 MAIN and W51 SOUTH) have no 20 μm counterparts to a level of 3 Jy (Genzel *et al.* 1982). Far-infrared observations show a bright ($3 \times 10^4$ Jy at 60 μm and 80 μm), 50–70 K, $\leq 20″$ diameter source approximately coincident with IRS 2 and extended far-IR emission covering most of the region of IRS 1. There is no apparent peak in far-IR brightness toward the other compact H II regions and maser centers. The emission from W51 MAIN has a 74 μm flux density of $\leq 6 \times 10^3$ Jy into a 30″ beam (Thronson and Harper 1979; Erickson and Tokunaga 1980; Harvey, Hoffmann, and Campbell 1975).

W51 is principally of interest as one of the class of most luminous regions in the galaxy containing newly formed stars. We have studied the structure and physical conditions of both the regions immediately around the newly formed O stars and of the more extensive molecular cloud. As part of a larger study, we have made a 40″ resolution submillimeter (sub-mm) continuum map of W51. Since the sub-mm emission is optically thin for $H_2$ column densities up to $10^{25}$ cm$^{-2}$ and since its strength is not strongly dependent on temperature, the sub-mm continuum map can tell us about the distribution of the material in the cloud. We will use the information derived from the sub-mm observations to study the molecular cloud and its relation to the sources of luminosity within it and to explain the absence of observable 20 μm sources toward the W51 MAIN and W51 SOUTH $H_2O$ emission centers.

## II. OBSERVATIONS

We made the observations of W51 on 1983 April 24 and 25 with the University of Chicago f/35 sub-mm photometer (Whitcomb, Hildebrand, and Keene 1980) on the 3.6 m Canada-France-Hawaii telescope on Mauna Kea, Hawaii. Scans of Saturn show that the 29 mm focal plane aperture used for the observations resulted in an approximately Gaussian beam with a full width to half-maximum of 42″. A low-frequency pass filter (Whitcomb and Keene 1980) and diffraction by the field optics and the telescope fixed the limits of the instrumental spectral passband at 300 μm and 800 μm. The flux-weighted mean wavelength at the measured line-of-sight water vapor (1–2 mm) was approximately 400 μm. We mapped the region by making beam-switched measurements at approximately 80 points separated by 20″. Most points were observed twice. The chopping telescope secondary gave a beam separation of 130″ north-south. The telescope was initially pointed by offsetting from a nearby SAO star and then moved while making the map using a focal plane offset guider.

[1]University of California, Berkeley, Space Sciences Laboratory.
[2]Visiting Astronomer, Canada-France-Hawaii Telescope, which is operated by the National Research Council of Canada, the Centre National de la Recherche Scientifique of France, and the University of Hawaii.
[3]Institute for Astronomy, University of Hawaii.
[4]Enrico Fermi Institute, Department of Astronomy and Astrophysics, and Department of Physics, University of Chicago.

We have determined the position of the sub-mm peak to $\pm 6''$. The position agrees with preliminary measurements of the peak of W51 made in 1980 July and September and 1982 November on the NASA-IRTF and UKIRT telescopes. The relative positions of the map grid points are known to approximately $\pm 2''$. We derived the absolute flux calibration from observations of Saturn assuming a 400 $\mu$m brightness temperature of 122 K (Hildebrand *et al.* 1984). The overall uncertainty in the absolute value of the peak flux density toward W51 is approximately 30%. Repeated observations of the peak of W51 while making the map resulted in a relative uncertainty of approximately $\pm 5\%$ of the peak flux for other points in the map.

### III. RESULTS

Figure 1 shows the sub-mm map of W51. The contour units are 0.1 of the peak value (1200 Jy per beam, $2.6 \times 10^{-16}$ W m$^{-2}$ Hz$^{-1}$ sr$^{-1}$ at 400 $\mu$m). This peak flux density is in good agreement ($\pm 10\%$) with the 350 $\mu$m value of Rieke *et al.* (1973) when source size, beam size, and wavelength corrections are applied. Figure 2 shows part of the sub-mm map superposed on the 20 $\mu$m map of Genzel *et al.* (1982). This figure also shows the positions of the H$_2$O maser emission centers and compact H II regions mentioned in § I. The sub-mm map shows a strong, approximately 40$''$ ($4 \times 10^{18}$ cm) diameter peak in the east coincident with the compact H II region W51e2 and the H$_2$O maser center W51 MAIN and distinctly separate from the extended H II region and near-IR source W51 IRS 1. About 1$'$ to the northwest, near the position of W51 IRS 2, is a secondary maximum with about half the intensity of the main peak. The distribution of 400 $\mu$m emission contrasts with the appearance of W51 at 74 $\mu$m where the more luminous source near IRS 2 ($4 \times 10^6$ $L_\odot$ vs. $1 \times 10^6$ $L_\odot$) dominates (Thronson and Harper 1979). There is a significant dropoff in sub-mm emission between the two peaks as indicated by the curvature of the intensity contours north and south of the saddle joining them. Given the beam
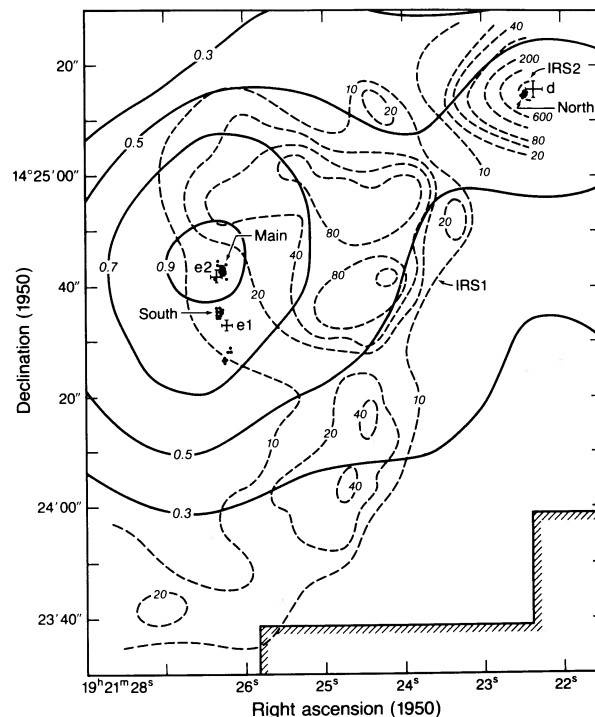


FIG. 2.—The dark lines show the sub-mm contours from Fig. 1. The dashed lines are the 20 $\mu$m continuum contours of Genzel *et al.* (1982). The crosses give the positions and sizes of the compact H II regions (Scott 1978; Genzel *et al.* 1982; Ho, Genzel, and Das 1983). The small dots represent the positions of H$_2$O maser features (Genzel *et al.* 1982).

size and the deconvolved sub-mm source sizes, the results are consistent with a complete absence of bridging emission between the two sources. The sub-mm surface brightness of the extended H II region and its associated 20 $\mu$m source (IRS 1) is probably less than 10% of the peak surface brightness.

Table 1 gives a listing of source parameters derived from the sub-mm map. We derived the 400 $\mu$m optical depth toward the peak (Jaffe *et al.* 1983) assuming an average dust temperature of 35 K derived from the data of Thronson and Harper (1979) and the present results. To derive peak values of $A_v$ and $n_{H_2}$, we assumed a Gaussian density profile and used the relationship between visual and sub-mm optical depth and between sub-mm optical depth and H$_2$ column density derived from the work of Whitcomb *et al.* (1981) (see Hildebrand 1983). If the distribution of material in W51 MAIN is more sharply peaked than a Gaussian, the derived values will be correspondingly higher. The relation between sub-mm optical depth and H$_2$ column density which was derived by Hildebrand (1983), $N_{H_2} \approx 6 \times 10^{24} \tau_{400}$, implies H$_2$ column densities approximately 3–10 times higher in a given source than those derived based on far-IR and submillimeter optical depth comparisons with (possibly optically thick) $^{13}$CO lines (Righini-Cohen and Simon 1977; Evans, Blair, and Beckwith 1977; Dickman 1978) and approximately 2 times lower than those estimated by Westbrook *et al.* (1976) from theoretical dust properties. The systematic uncertainties in the Hildebrand (1983) result (a factor of 2) are considerably lower than those in the earlier work.
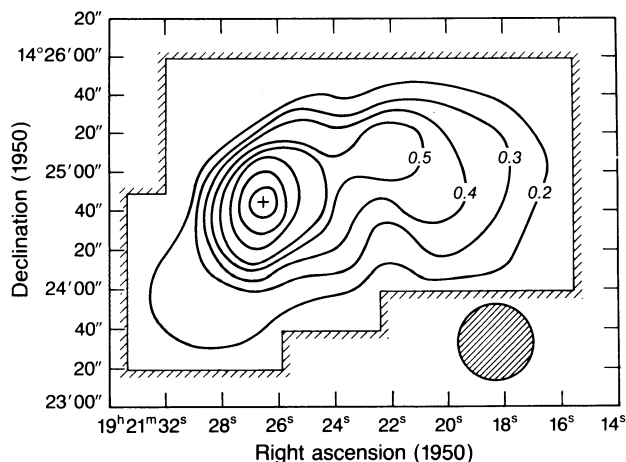


FIG. 1.—Submillimeter map of W51. The contour levels are 0.2, 0.3, 0.4, 0.5, 0.6, 0.7, 0.8, and 0.9 of the peak flux. The cross denotes the position of the peak. The peak 400 $\mu$m flux density is 1200 Jy per beam corresponding to a surface brightness of $2.6 \times 10^{-16}$ W m$^{-2}$ Hz$^{-1}$ sr$^{-1}$.

TABLE 1

SUBMILLIMETER RESULTS

| Parameter | Value |
|---|---|
| Position $\alpha(1950)$, $\delta(1950)$: | |
| Peak 400 $\mu$m ............. | $19^h21^m26\overset{s}{.}4$, $+14°24'44'' \pm 6''$ |
| $H_2O$ MAIN[a] ............. | $19^h21^m26\overset{s}{.}21 \pm 0\overset{s}{.}01$, $+14°24'42''.9 \pm 0''.2$ |
| Secondary maximum...... | $19^h21^m22\overset{s}{.}0 \pm 0\overset{s}{.}6$, $+14°25'11'' \pm 9''$ |
| $H_2O$ NORTH[a] .......... | $19^h21^m22\overset{s}{.}40 \pm 0\overset{s}{.}01$, $+14°25'12''.9 \pm 0''.2$ |
| Deconvolved 400$\mu$m size ... | $40'' \pm 7''$ |
| Peak 400 $\mu$m optical depth ............. | 0.17 |
| Peak column density ($N_{H_2}$) ............ | $1.0 \times 10^{24}$ cm$^{-2}$ |
| Peak $A_v$...................... | 1000 |
| Peak density ($n_{H_2}$) ......... | $2.2 \times 10^5$ |
| Mass in central beam ....... | $2.4 \times 10^4$ $M_\odot$ |
| Total mass .................. | $9.4 \times 10^4$ $M_\odot$ |

[a] Moran et al. 1981, as quoted by Ho, Genzel, and Das 1981.

IV. DISCUSSION

The peak of the sub-mm emission in W51 coincides with the $H_2O$ emission center W51 MAIN and the compact H II region W51e2 and is significantly distinct from the other noteworthy molecular, infrared, and radio continuum features in the region. One exception is the high-excitation $J = 4-3$ transition of HCN which peaks near the sub-mm position and has a slightly broader distribution (White et al. 1982). The total mass in this main peak is very large: $5 \times 10^4$ $M_\odot$ in a $40''$ diameter Gaussian source. This is comparable to the mass of many 50–100 pc long giant molecular clouds but is compacted into only a 1.4 pc area (Stark and Blitz 1978; Blitz 1980). The total mass of the material in the sub-mm emission region is approximately $10^5$ $M_\odot$ which is $10^2$–$10^3$ times larger than the masses of the molecular cloud cores in OMC-1, W3, and S255 as measured by the sub-mm method (Keene, Hildebrand, and Whitcomb 1982; Jaffe et al. 1983, 1984). The central region of W51 occupies a volume that is also approximately $10^2$ times larger than the core volumes of these sources leading to a density comparable to the densities obtained for the more nearby sources. Averaged over 1.4 pc, the sub-mm results imply $n_{H_2} \sim 2 \times 10^5$ cm$^{-3}$. As discussed in § III, the actual densities at the core of the source are probably higher. The presence of this extensive dense core supports the suggestion of Ho, Genzel, and Das (1983) that the hot, $NH_3$ emission arises in the turbulent region where the massive outflows from the stars powering the $H_2O$ emission centers (Genzel et al. 1981; Schneps et al. 1981) collide with surrounding quiescent gas. The mass and density imply that the core of the source has a mass greater than 500 times its Jeans mass. Even in the presence of substantial impediment to collapse in the form of strong magnetic fields or turbulence generated by stellar winds, a large number of stars should form in this region in a short time ($\tau_{free\ fall} \sim 10^5$ yr). A 1% star formation efficiency will result in an approximately 500

$M_\odot$ cluster concentrated in an approximately 1 pc$^3$ volume. Preliminary sub-mm investigations indicate that other distant $H_2O$ maser emission centers like W49 have comparable mass concentrations in their cores.

The secondary sub-mm maximum near IRS 2 is both hotter (as implied by the far-IR results) and fainter in the sub-mm than the peak at W51 MAIN. The size of this secondary peak is difficult to determine both because of its proximity to the main peak and because of the possibility that it sits atop a plateau of diffuse emission from the entire molecular cloud. Nevertheless, the flux and the temperature of this source imply that it has almost an order of magnitude less mass than W51 MAIN ($\leq 10^4$ $M_\odot$), even though its luminosity is about 4 times larger.

The hot dust around the stars that power the $H_2O$ maser emission centers, compact H II regions, and warm $NH_3$ clumps near the peak of the sub-mm source must emit copious amounts of 10–20 $\mu$m radiation ($S_\nu$ [20 $\mu$m] $\sim$ a few thousand Jy if all the luminosity emerges from an unextincted 200 K blackbody). The sub-mm results presented here provide a simple explanation for the nondetection of this radiation. We derive a visual extinction, $A_v$, toward the sub-mm peak of 1000. For interstellar dust, the ratio of $A_v$ to 2.2 $\mu$m extinction, $A_K$, is approximately 11 (Johnson 1968). Toward the galactic center, the observed extinction curve gives a 20 $\mu$m extinction, $A_{20} = 1/3$ $A_K$ (Becklin et al. 1978). The high empirical value is probably due to a silicate feature present in the 20 $\mu$m band. We can obtain a reasonable lower bound for $A_{20}$ by assuming that the extinction is inversely proportional to wavelength in the near-IR. This gives $A_{20} = 1/9$ $A_K$. These two 20 $\mu$m extinction relations imply $A_{20} = 10$–30 toward the sum-mm peak. Alternatively, we can estimate $A_{20}$ directly from the peak 400 $\mu$m optical depth $\tau_{400} = 0.17$. If we assume $\tau_\lambda \propto \lambda^{-2}$ for $\lambda \geq 200$ $\mu$m and $\propto \lambda^{-1}$ for $\lambda < 200$ $\mu$m, we obtain $A_{20} = 7.4$. The peak $A_{20}$ toward W51 IRS 2 is less than one-fourth of the value toward the main sub-mm peak. As a result, if all sources are halfway through the cloud, a given 20 $\mu$m source would appear, on average, 30–$10^6$ times brighter if it were at the center of the secondary sub-mm peak than if it were at the center of the main peak.

Almost all strong maser emission centers have closely associated 20 $\mu$m counterparts (Downes et al. 1984). These counterparts are generally 10–100 times fainter than the well-studied near-IR sources in other strong star formation regions. The present results in W51 indicate that the low 20 $\mu$m fluxes of these sources may result from large amounts of cool overlying dust rather than from intrinsic properties of the sources.

REFERENCES

Becklin, E. E., Matthews, K., Neugebauer, G., and Willner, S. P. 1978, Ap. J., 220, 831.
Bieging, J. H. 1975, in H II Regions and Related Topics, ed. T. L. Wilson and D. Downes (Berlin: Springer-Verlag), p. 443.
Blitz, L. 1980, in Giant Molecular Clouds in the Galaxy, ed. P. M. Solomon and M. G. Edmunds (Oxford: Pergamon), p. 1.
Dickman, R. L. 1978, Ap. J. Suppl., 37, 407.

Downes, D., Becklin, E. E., Genzel, R., and Wynn-Williams, C. G. 1984, in preparation.

Downes, D., Wilson, T. L., Bieging, J., and Wink J. 1980, *Astr. Ap.*, **79**, 233.

Erickson, E. F., and Tokunaga, A. T. 1980, *Ap. J.*, **238**, 596.

Evans, N. J., Blair, G. N., and Beckwith, S. 1977, *Ap. J.*, **217**, 448.

Forster, J. R., Welch, W. J., Wright, M. C. H., and Baudry, A. 1978, *Ap. J.*, **221**, 137.

Genzel, R., Becklin, E. E., Wynn-Williams, C. G., Moran, J. M., Reid, M. J., Jaffe, D. T., and Downes, D. 1982, *Ap. J.*, **255**, 527.

Genzel, R., Downes, D., Schneps, M. H., Reid, M. J., Moran, J. M., Kogan, L. R., Kostenko, V. I., Matveyenko, L. I., and Rönnäng, B. 1981, *Ap. J.*, **247**, 1039.

Harvey, P. M., Hoffmann, W. F., and Campbell, M. F. 1975, *Ap. J. (Letters)*, **196**, L31.

Hildebrand, R. H. 1983, *Quart. J. R. A. S.*, **24**, 267.

Hildebrand, R. H., Loewenstein, R. F., Harper, D. A., Keene, J. B., Orton, G. S., and Whitcomb, S. E. 1984, in preparation.

Ho, P. T. P., Genzel, R., and Das, A. 1983, *Ap. J.*, **266**, 596.

Jaffe, D. T., Davidson, J. A., Dragovan, M., and Hildebrand, R. H. 1984, *Ap. J.*, submitted.

Jaffe, D. T., Hildebrand, R. H., Keene, J., and Whitcomb, S. E. 1983, *Ap. J. (Letters)*, **273**, L89.

Johnson, H. L. 1968, in *Stars and Stellar Systems*, Vol. **7**, *Nebulae and Interstellar Matter*, ed. B. M. Middlehurst and L. H. Allen (Chicago: University of Chicago Press), p. 167.

Keene, J., Hildebrand, R. H., and Whitcomb, S. E. 1982, *Ap. J. (Letters)*, **252**, L11.

Rieke, G. H., Harper, D. A., Low, F. J., and Armstrong, K. R. 1973, *Ap. J. (Letters)*, **183**, L67.

Righini-Cohen, G., and Simon, M. 1977, *Ap. J.*, **213**, 390.

Schneps, M. H., Lane, A. P., Downes, D., Moran, J. M., Genzel, R., and Reid, M. J. 1981, *Ap. J.*, **249**, 124.

Scott, P. F. 1978, *M. N. R. A. S.*, **183**, 435.

Stark, A. A., and Blitz, L. 1978, *Ap. J. (Letters)*, **225**, L15.

Thronson, H. A., and Harper, D. A. 1979, *Ap. J.*, **230**, 133.

Westbrook, W. E., Werner, M. W., Elias, J. H., Gezari, D. Y., Hauser, M. G., Lo, K. Y., and Neugebauer, G. 1976, *Ap. J.*, **209**, 94.

Whitcomb, S. E., Gatley, I., Hildebrand, R. H., Keene, J., Sellgren, K., and Werner, M. W. 1981, *Ap. J.*, **246**, 416.

Whitcomb, S. E., Hildebrand, R. H., and Keene, J. 1980, *Pub. A.S.P.*, **92**, 863.

Whitcomb, S. E., and Keene, J. 1980, *Pub. A.S.P.*, **92**, 863.

White, G. J., Phillips, J. P., Beckman, J. E., and Cronin, N. J. 1982, *M. N. R. A. S.*, **199**, 375.

Wynn-Williams, C. G., Becklin, E. E., and Neugebauer, G. 1974, *Ap. J.*, **187**, 473.

E. E. BECKLIN: University of Hawaii, Institute for Astronomy, 2680 Woodlawn Drive, Honolulu, HI 96822

R. H. HILDEBRAND: University of Chicago, Enrico Fermi Institute, 5630 South Ellis Avenue, Chicago, IL 60637

D. T. JAFFE: University of California, Space Sciences Laboratory, Berkeley, CA 94720